VSP

Journal of Biomaterials Science 20 (2009) 1369–1380

Journal of BIOMATERIALS SCIENCE
www.brill.nl/jbs

Preparation and Therapeutic Efficacy of Polysorbate-80-Coated Amphotericin B/PLA-b-PEG Nanoparticles

Tianbin Ren [a], **Nan Xu** [b], **Chunhong Cao** [a], **Weizhong Yuan** [a], **Xiao Yu** [a], **Jianghan Chen** [b] **and Jie Ren** [a,*]

[a] Institute of Nano and Bio-Polymeric Materials, School of Material Science and Engineering, Tongji University, Shanghai 200092, P. R. China

[b] Department of Dermatology, Changzheng Hospital, Second Military Medical University, Shanghai 200003, P. R. China

Received 21 April 2008; accepted 24 July 2008

Abstract

Amphotericin B (AmB)/poly(lactic acid)-b-poly(ethylene glycol) (PLA-b-PEG) nanoparticles coated with polysorbate 80 (Tween-80) were prepared by nanoprecipitation for transport across the blood–brain barrier (BBB). The effects of Tween-80 on the size and distribution, entrapment efficiency and release behavior of AmB/PLA-b-PEG nanoparticles were investigated. Furthermore, the brain targeting and curative effect of coated nanoparticles were also investigated. The entrapment efficiency was significantly enhanced when nanoparticles were coated with Tween-80. The prepared nanoparticles were spherical with homogeneous distribution. Drug concentration in mice brain was greatly enhanced, which indicated that the coated nanoparticles could get across the BBB. Meanwhile, the AmB/PLA-b-PEG nanoparticles are able to reduce the toxicity of AmB to liver, kidney and blood system with improved therapeutic effect.

Keywords

AmB/PLA-b-PEG, nanoparticles, polysorbate 80, cryptococcal meningitis, blood–brain barrier

1. Introduction

Cryptococcal meningitis, caused by *Cryptococcus neoformans*, is an infection of the meninges (the membranes covering the brain and spinal cord). In recent years, the incidence of cryptococcal meningitis has increased dramatically, especially in immunocompromised patients, including those with AIDS, while the survival rate is often low. Amphotericin B (AmB) is the preferred drug for the treatment of cryp-

* To whom correspondence should be addressed. E-mail: renjie6598@163.com

 DOI:10.1163/092050609X12457418779185

tococcal meningitis by selectively binding to ergosterol and disrupting the fungal membrane, resulting in leakage of the intracellular contents and cellular death [1]. However, the efficiency of the drug is limited because of its serious toxicity and side-effects such as fever, headache, chills, vomiting and so forth [2, 3]. Besides, the blood–brain barrier (BBB) is an obstacle for AmB to penetrate brain tissue to reach the central nervous system (CNS) where the pathogen is located [4, 5].

Different methods have been developed to enhance drug delivery to the brain [6, 7]. Using liposomes as drug-delivery system is an attractive idea and a number of trials have been made to improve their efficacy by enhancing the liposomal affinity to the brain capillary endothelial cells [8–10]. Liposomal amphotericin B (AmBisome), adhering to endothelial cell membrane and subsequent releasing AmB into the cells, was then applied because of the reduced toxicity of AmB. However, most experiments in this area failed to show a remarkable efficacy [11, 12].

Polymer nanoparticles, especially when coated with a surfactant, have attracted considerable interest for drug-delivery systems [13–18]. A lot of surfactants were investigated to compare their efficacy in transporting drug across the BBB. Kreuter *et al.* showed that Tween-80 was the most effective and coating nanoparticles with Tween-80 led to the uptake by the brain capillary endothelial cells [19]. It was also reported that nanoparticles coated with Tween-80 could get across the BBB and enhance the brain drug concentration 20–60-fold [20–22].

Poly(lactic acid) (PLA) and its co-polymers are widely used in medical applications because of their biodegradability, low toxicity and good mechanical properties [23–25]. Among them, poly(lactic acid)-b-poly(ethylene glycol) (PLA-b-PEG) appeared to be an excellent drug carrier due to its low tissue toxicity, few side-effects and a controllable drug release rate. Furthermore, the PLA-b-PEG nanoparticles can reduce the uptake by the mononuclear phagocytic system (MPS) *in vivo* compared to the unmodified PLA.

In the present study, PLA-b-PEG co-polymer nanoparticles coated with Tween-80 were prepared as an anti-cryptococcosis carrier for controlled release of AmB because of their biodegradability, biocompatibility, low toxicity and specified penetrability of the BBB. The effects of Tween-80 on nanoparticle size, entrapment efficiency and release behavior were also investigated. In addition, the efficacy and side-effect of AmB/PLA-b-PEG nanoparticles were studied by animal testing.

2. Materials and Methods

2.1. Materials

Poly(ethylene glycol) (PEG) with a number-average molecular weight of 4000 g/mol was used after drying *in vacuo* at 80°C for more than 10 h. D,L-Lactide (LA) was used after further purification. PLA-b-PEG co-polymer was produced by the ring-opening polymerization of D,L-lactide with a certain amount of PEG (LA/PEG = 8:1 (w/w)) [26]. AmB was obtained from Pioneer Pharmaceutical (Shanghai, P. R. China). PEG, polysorbate 80 (Tween-80), anhydrous methanol

and dimethylsulfoxide were purchased from Sinopharm Chemical (Shanghai, P. R. China). All other reagents were AR grade.

Healthy mice weighing 20–30 g (provided by Laboratory Animal Center of the Second Military Medical University, Shanghai, China) were used in the *in vivo* study. The animals got water and food freely. All procedures were in accordance with the requirements of the National Act on the use of experimental animals (China).

2.2. Preparation of AmB/PLA-b-PEG Nanoparticles

AmB/PLA-b-PEG nanoparticles were prepared by nanoprecipitation [27]. The process was described as follows: 400 mg of PLA-b-PEG co-polymer and 2 mg of AmB were dissolved in a mixture of 20 ml acetone and 0.5 ml dimethylsulfoxide (DMSO), and then the solution was added drop-wise under constant stirring to 20 ml of Tween-80 aqueous solution in a beaker. Then the beaker with solution was covered with aluminum foil with some holes. Acetone was evaporated at room temperature for more than 3 days.

2.3. Nanoparticle Size Analysis

The nanoparticle suspension was homogenized by ultrasound for 20 min. Then nanoparticle size and size distribution were measured by laser light scattering (LS230, Beckman Coulter, USA) at 25°C.

2.4. Entrapment Efficiency Assay

AmB was dissolved in DMSO, and then the solution was diluted to obtain AmB solutions with different concentrations. The solutions of AmB were examined by UV spectrometer (U-1860, Hitachi, Japan) at a wavelength of 415 ± 1 nm to obtain the calibration curve of drug.

40 mg of freeze-dried AmB-loaded nanoparticles were dialyzed in methanol to separate the free AmB until the absorbance at 415 nm was zero. Then these nanoparticles were incubated in 50 ml DMSO at 60°C for 2 h. The solution was measured spectrophotometrically at 415 ± 1 nm and the AmB concentration (by weight) was determined according to the calibration curve [28]. The entrapment efficiency of AmB was calculated as follows:

$$\text{Entrapment efficiency (\%)} = (\text{Weight of AmB loaded}/\text{Weight of AmB incorporated}) \times 100.$$

2.5. Nanoparticle Morphology

The nanoparticle suspensions were homogenized by ultrasound. Then a drop of nanoparticle suspension (concentration is below 1:1000) was loaded onto a copper halftone and then dyed by 1% (wt) phosphotungstic acid solution. The sample was characterized by H-600 TEM (Hitachi, Japan) at a 75 kV electron beam accelerating voltage.

2.6. In Vitro *Release*

The calibration curve was obtained as above. Nanoparticles were dialyzed against phosphate-buffered saline solution (PBS, pH 7.4) in a water bath at 37°C. Samples were taken out from release medium at certain time intervals and measured spectrophotometrically at 409 ± 1 nm. The accumulated concentration was calculated in accordance with the calibration curve.

2.7. *The Analysis of AmB Concentrations* in Vivo

Tween-80-coated AmB/PLA-b-PEG nanoparticles and AmB injectable powder were administered intravenously to mice through tail vein. The AmB concentrations *in vivo* were analyzed by high-performance liquid chromatography (HPLC, Dikma-C18, Dikma EasyGuard, Dikma, USA) of 20-μl samples at 37°C. The mobile phase was acetonitrile/water (40:60, v/v) and 4% acetic acid, the flow rate was 0.9 ml/min. Drug concentrations were determined spectrophotometrically at 405 nm.

2.8. *Preparation of* Cryptococcus Neoformans *Suspension*

Cryptococcus neoformans placed on Sabourand's medium was incubated under sterile conditions for 3 days at 37°C. A final fungal suspension of 5.0×10^8 cfu/ml was obtained by dissolving the colony into normal saline, after which the concentration on the counting plate under the microscope was calculated. The prepared suspension was used within 1 h.

2.9. *Cryptococcal Meningitis-Bearing Mice*

BALB/c mice were anesthetized with ethyl ether and then injected with *Cryptococcus neoformans* suspension through the foramen magnum 24 h after an intraperitoneal injection of cyclophosphamide for immunoimpression (concentration 10 mg/ml, dose 10 μl/g live weight). The treated mice were fed normally and their survival times were recorded.

The cryptococcal meningitis-bearing mice were divided into three groups with 20 animals per group; the following preparations were injected through the tail vein: (1) AmB injectable powder (1 mg/kg); (2) AmB/PLA-b-PEG nanoparticles coated with Tween-80 (6 mg/kg AmB); or (3) normal saline (0.1 ml).

2.10. *Animal Tissue Samples*

At 12 h, 1, 3, 5 and 7 days post-injection, mice were killed and then perfused with paraformaldehyde. The organs were collected and sectioned after perfusion; hematoxylin and eosin-stained sections were observed under a microscope.

2.11. *Fungal Culture*

The brain of mice was completely milled with normal saline in a disinfected grinder. The homogenates were evenly laid on Sabourand's medium and incubated at 37°C. Fungal growth was recorded at specific intervals.

2.12. The Effect of Tween-80-Coated Nanoparticles on Marrow, Liver and Kidney

The cryptococcal meningitis-bearing mice were divided into 4 groups of 10 animals per group.

Mice in each group were treated by tail vein injection of (1) AmB injectable powder (1 mg/kg); (2) AmB/PLA-b-PEG nanoparticles coated with Tween-80 (6 mg/kg); (3) PLA-b-PEG nanoparticles (6 mg/kg); or (4) Tween-80 (1%).

The orbital blood of mice was obtained at 24 h before and after administration and again at 7 days after continuous administration every day. Then 1 ml orbital blood was collected into EDTA-anticoagulant tube for blood routine determination. Obtained serum from centrifuged blood (14 000 rpm for 10 min) were stored at −20°C for the blood enzyme test.

The indices of red blood cells (RBC), white blood cells (WBC), platelets (PLT), alanine aminotransferase (ALT), aspartate aminotransferase (AST), blood urea nitrogen (BUN) and creatinine (Cr) were examined.

3. Results and Discussion

3.1. Size and Entrapment Efficiency of the Nanoparticles

The nanoparticle size and entrapment efficiency are shown in Table 1. These data showed that Tween-80, an excellent surfactant, is able to strengthen the stability of nanoparticles; however, the nanoparticle size increases slightly because of the absorption of Tween-80. The addition of surfactant lowered the surface tension of oil and water, which resulted in an increase in entrapment efficiency. On the other hand, AmB has a better solubility in DMSO than methanol; therefore, high entrapment efficiency can be obtained with small amounts of DMSO.

3.2. Morphology of Nanoparticles

The TEM observation shows that nanoparticles prepared by nanoprecipitation are spherical in shape and their distribution is homogeneous (Fig. 1). The nanoparticle size is within 100 nm.

Table 1.
The effect of co-solvent and surfactant on size and entrapment efficiency of nanoparticle*

Nanoparticle type	Co-solvent	Surfactant	Diameter (nm)	Entrapment efficiency (%)
Blank nanoparticle	–	–	114 ± 16	–
Blank nanoparticle	Methanol	Tween-80	130 ± 18	–
Blank nanoparticle	DMSO	Tween-80	118 ± 18	–
Drug nanoparticle	Methanol	–	131 ± 17	23.6
Drug nanoparticle	Methanol	Tween-80	133 ± 17	36.5
Drug nanoparticle	DMSO	–	120 ± 17	42.5
Drug nanoparticle	DMSO	Tween-80	120 ± 16	50.7

* The concentration of Tween-80 was 0.8%.

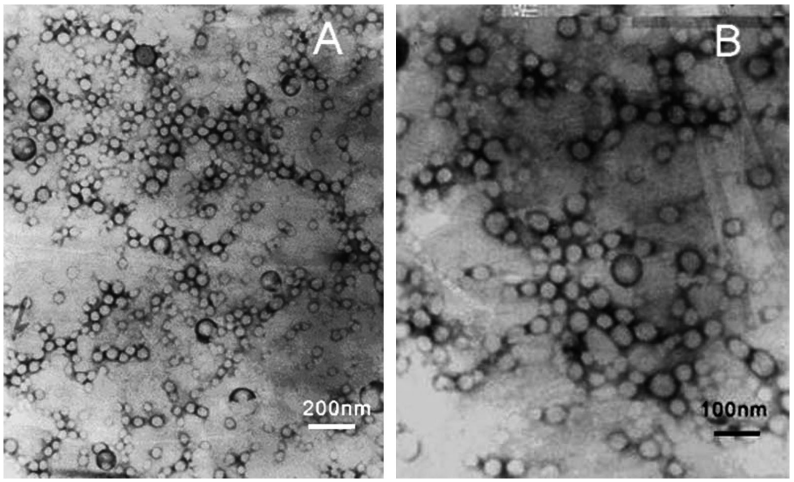

Figure 1. TEM images of Tween-80-coated AmB/PLA-b-PEG nanoparticles (co-solvent: DMSO).

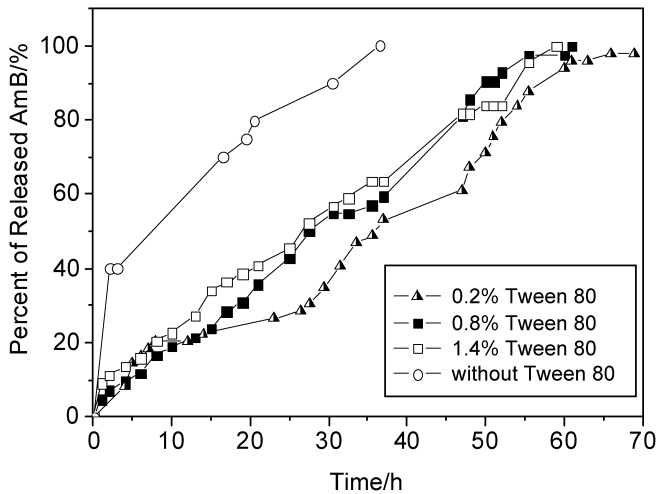

Figure 2. The effect of Tween-80 content on AmB release *in vitro*.

3.3. Drug Release in Vitro *of Nanoparticles Coated with Tween-80*

The release behavior of nanoparticles coated with 0.2%, 0.8% and 1.4% Tween-80 is similar (Fig. 2). Obviously, although the addition of Tween-80 could enhance the entrapment efficiency of nanoparticles, the effect on the release of AmB is not remarkable.

3.4. Brain Targeting of AmB/PLA-b-PEG Nanoparticles

AmB injectable powder (1 mg/kg) and Tween-80-coated AmB/PLA-b-PEG nanoparticles, respectively, were injected into mice. Changes of brain drug concentration at 0.5–48 h after injection showed noticeable brain targeting of AmB/PLA-b-PEG

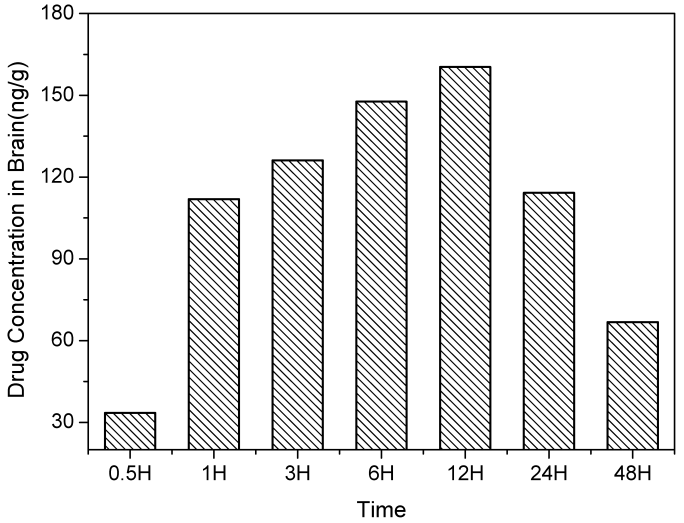

Figure 3. Drug concentration of nanoparticles in brain over time after administration of AmB/PLA-b-PEG nanoparticles.

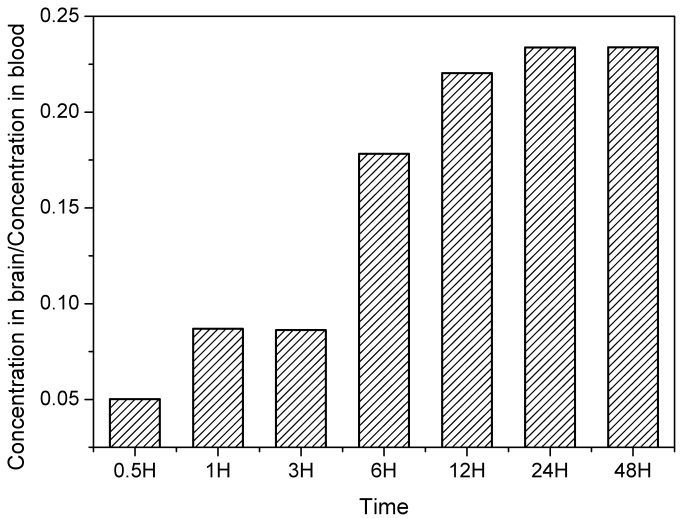

Figure 4. Brain/blood drug concentration ratio over time after administration of AmB/PLA-b-PEG nanoparticles.

nanoparticles (Figs 3 and 4). It has been reported that a small amount of AmB injectable powder could get across the BBB into the brain; however, we could not detect it because of low instrument sensitivity.

It has been reported in the literature that PLA nanoparticles coated with Tween-80 could pass through the BBB [29]. Recently, some authors observed the distribution of PLA nanoparticles in the brain of mice under a fluorescence microscope,

TEM and analytic electron microscope (AEM) to confirm the BBB penetration of Tween-80-coated PLA nanoparticles. The experiments suggested that one of the mechanisms may be the endocytosis by the endothelial cells of brain blood vessels [30, 31]. All these results showed that AmB/PLA-b-PEG nanoparticles coated with Tween-80 has the ability of brain-targeting.

3.5. Efficacy of Tween-80-Coated AmB/PLA-b-PEG Nanoparticles

To investigate the lifespan of mice with different treatments the survival time was statistically analyzed.

Most mice administered more than 1 mg/kg AmB would die, while the nanoparticle-bound AmB could reach 6 mg/kg. Obviously, the toxicity of AmB encapsulated in nanoparticle was significantly lower.

The survival time of mice receiving AmB/PLA-b-PEG nanoparticles is twice that of the other two groups. It indicates that the AmB/PLA-b-PEG nanoparticles are able to pass through the BBB, while the AmB injectable powder cannot (Fig. 5).

The recovery of *Cryptococcus neoformans* form the brain of mice under different treatments also supports this conclusion (Table 2). The colony growth speed of the AmB group is much higher than that of AmB/PLA-b-PEG nanoparticles group. The colony count of the former is significantly higher than that of the latter. These phenomena further confirmed the therapeutic efficacy of Tween-80-coated AmB/PLA-b-PEG nanoparticles in fungal infection in the brain. The mechanism will be explored in our further work.

3.6. The Liver, Kidney and Blood System Indices

In order to examine the adverse effects of different treatments, the liver, kidney and blood system indices were measured (Tables 3–5). According to these data,

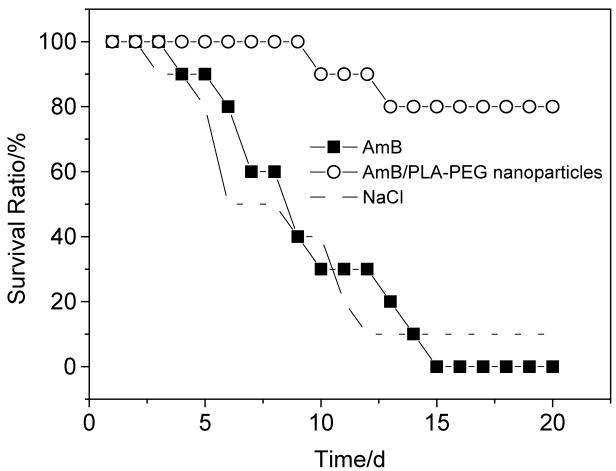

Figure 5. The survival ratio of *Cryptococcus neoformans*-infected mice under different treatments.

Table 2.
Recovery of *Cryptococcus neoformans* from the brain of mice with AmB, Tween-80-coated AmB/PLA-b-PEG nanoparticles and NaCl treatment

Treatment	Dose	Colony counts $\log_{10}$ (mean cfu/g ± SEM)	
		1 day	7 days
AmB	1 mg/kg	5.51 ± 0.03	5.73 ± 0.02
NaCl	0.1 ml	5.63 ± 0.07*	5.74 ± 0.05
AmB-PLA/PEG-NP	6 mg/kg	4.68 ± 0.07*	3.96 ± 0.05*

* $P < 0.05$, compared with AmB group.

Table 3.
The blood index of mice under different treatments

		Before administration	After administration	
			1 day	7 days
AmB	WBC	8.4 ± 1.90	16.48 ± 3.62^{a}	18.84 ± 2.80^{a}
	RBC	5.84 ± 0.37	4.302 ± 0.34^{a}	3.3 ± 0.37^{ac}
	HGB	147.8 ± 5.11	106.4 ± 8.14^{a}	88.6 ± 7.63^{ac}
	PLT	863.2 ± 120.82	1179 ± 98.23^{a}	1331.4 ± 92.56^{ac}
Tween-80-coated AmB/PLA-b-PEG nanoparticle	WBC	6.63 ± 1.24	7.32 ± 1.63	7.56 ± 0.98
	RBC	6.142 ± 0.55	6.38 ± 0.35	6.14 ± 0.18
	HGB	148.8 ± 8.42	146.2 ± 7.63	142.2 ± 3.97
	PLT	935.2 ± 113.12	923.4 ± 80.01	935.2 ± 44.29
Blank nanoparticles	WBC	5.92 ± 1.15	7.44 ± 2.24	7.16 ± 1.69
	RBC	6.32 ± 0.42	6.02 ± 0.60	5.69 ± 0.43^{bd}
	HGB	150.2 ± 16.29	142.4 ± 15.33	148 ± 22.35
	PLT	5.92 ± 1.15	7.44 ± 2.24	7.16 ± 1.69
Tween-80	WBC	7.6 ± 1.83	7.8 ± 1.93	8.16 ± 1.97
	RBC	6.18 ± 0.65	6.186 ± 0.42	6.132 ± 0.74
	HGB	140.8 ± 10.76	137.4 ± 9.77	140.4 ± 11.41
	PLT	950.8 ± 69.74	1006.2 ± 57.79	987.8 ± 45.69

[a] $P < 0.01$, compared with before treatment.
[b] $P < 0.05$, compared with before treatment.
[c] $P < 0.01$, compared with 1 day after treatment.
[d] $P < 0.05$, compared with 1 day after treatment.

no obvious side-effects on blood, liver and kidney were observed after injection of blank nanoparticles or Tween-80 alone. AmB/PLA-b-PEG nanoparticles were able to escape the uptake by phagocytic cells of the liver, spleen and reticuloendothelial system (RES); therefore, the accumulation of AmB in liver and spleen decreased compared to AmB powder injection. The accumulation of drug in the kidney is

Table 4.
The liver index of mice under different treatments

		Before administration	After administration	
			1 day	7 days
AmB	ALT	638.6 ± 115.18	1059.2 ± 119.2[a]	1755 ± 175.39[ab]
	AST	1634.2 ± 193.55	2466.6 ± 357.30[a]	2684.2 ± 494.74[a]
Tween-80-coated AmB/PLA-b-PEG nanoparticle	ALT	709.2 ± 111.87	758.6 ± 145.34	772.2 ± 191.40
	AST	1722 ± 84.73	1736.8 ± 162.27	1746.2 ± 87.64
Blank nanoparticles	ALT	730.6 ± 105.6	757.2 ± 81.58	783.4 ± 38.84
	AST	1623.4 ± 154.71	1677 ± 272.8	1652.2 ± 139.42
Tween-80	ALT	787.4 ± 87.39	811 ± 99.02	803 ± 118.19
	AST	1647.8 ± 170.62	1581.4 ± 181.85	1717 ± 155.76

[a] $P < 0.01$, compared with before treatment.
[b] $P < 0.01$, compared with 1 day after treatment.

Table 5.
The kidney index of mice under different treatments

		Before administration	After administration	
			1 day	7 days
AmB	BUN	6.008 ± 0.67	7.56 ± 0.55[a]	9.97 ± 0.59[ac]
	CREA	17.64 ± 3.59	22.98 ± 3.95	23.8 ± 3.28
Tween-80-coated AmB/PLA-b-PEG nanoparticles	BUN	6.13 ± 0.51	6.49 ± 0.72	6.88 ± 0.47
	CREA	15.64 ± 2.25	15.56 ± 2.56	15.92 ± 2.26
Blank nanoparticles	BUN	6.89 ± 0.66	6.61 ± 0.92	6.83 ± 1.32
	CREA	15.96 ± 1.98	15.92 ± 1.82	15.82 ± 1.99
Tween-80	BUN	7.12 ± 1.00	6.92 ± 0.99	6.78 ± 1.05
	CREA	16.38 ± 1.54	16.54 ± 1.79	17.68 ± 0.79[bd]

[a] $P < 0.01$ compared with before treatment.
[b] $P < 0.05$, compared with before treatment.
[c] $P < 0.01$, compared with 1 day after treatment.
[d] $P < 0.05$, compared with 1 day after treatment.

also reduced because of the lowered filtration through the renal tubules. The drugs are simultaneously absorbed into nanoparticles evenly, stably and released slowly; consequently, the direct integration of AmB and cholesterol, existing in the surface of erythrocytes, is reduced effectively, so that the toxicity of AmB to erythrocytes is significantly reduced.

4. Conclusion

AmB/PLA-b-PEG nanoparticles were prepared by nanoprecipitation. According to the TEM images, nanoparticles coated with Tween-80 are spherical in shape and distributed uniformly. The average size was about 100 nm. The addition of Tween-80 strengthens the stability of nanoparticles and enhances the entrapment efficiency of AmB. Furthermore, investigation showed that the content of Tween-80 has little effects on the release properties.

According to animal testing, drug-loaded nanoparticles have brain targeting activity and the ability to get across the BBB to the CNS. More importantly, the AmB/PLA-b-PEG nanoparticles are able to reduce the toxicity of AmB to blood, liver and kidney, and improve the therapeutic effect.

Acknowledgement

This work was supported by Key Basic Research Foundation for development of Science and Technology of Shanghai, China (Project No. 05DJ14006).

References

1. T. J. Walsh and A. Pizzo, *Eur. J. Clin. Microbiol. Infect. Dis.* **7**, 460 (1988).
2. A. Pathak, F. D. Pien and L. Carvalho, *Clin. Infect. Dis.* **26**, 334 (1998).
3. G. Inselmann, U. Inselmann and H. T. Heidemann, *Eur. J. Intern. Med.* **13**, 228 (2002).
4. R. Kassab, H. Parrot-Lopez, H. Fessi, J. Menaucourt, R. Bonaly and J. Coulon, *Bioorg. Med. Chem.* **10**, 1767 (2002).
5. U. Fagerholm, *Drug Discov. Today* **12**, 1076 (2007).
6. K. Sachs-Barrable, S. D. Lee, E. K. Wasan, S. J. Thornton and K. M. Wasan, *Adv. Drug Deliv. Rev.* **60**, 692 (2008).
7. L. S. S. Guo, *Adv. Drug Deliv. Rev.* **47**, 149 (2001).
8. M. T. Krauze, J. Forsayeth, J. W. Park and K. S. Bankiewicz, *Pharm. Res.* **23**, 2493 (2006).
9. U. S. Sharma, A. Sharma, R. I. Chau and R. M. Straubinger, *Pharm. Res.* **14**, 992 (1997).
10. A. M. Abraham and A. Walubo, *Int. J. Antimicrob. Agents* **25**, 392 (2005).
11. E. W. M. van Etten, W. van Vianen, R. H. G. Tijhuis, G. Storm and I. A. J. M. Bakker-Woudenberg, *J. Control. Rel.* **37**, 123 (1995).
12. R. N. Kotwani, P. C. Gokhale, P. V. Bodhe, B. G. Kirodian, N. A. Kshirsagar and S. K. Pandya, *Int. J. Pharm.* **238**, 11 (2002).
13. T. Verrecchia, G. Spenlehaue, D. V. Bazile, A. Murry-Brelier, Y. Archimbaud and M. Veillard, *J. Control. Rel.* **36**, 49 (1995).
14. J. Keuter, R. N. Alyautdin, D. A. Kharkevich and A. A. Ivanov, *Brain. Res.* **674**, 171 (1995).
15. M. S. Espuelas, P. Legrand, J. M. Irache, C. Gamazo, A. M. Orecchioni, J.-Ph. Devissaguet and P. Ygartua, *Int. J. Pharm.* **158**, 19 (1997).
16. W. Q. Sun, C. S. Xie, H. F. Wang and Y. Hu, *Biomaterials* **25**, 3065 (2004).
17. J. M. Anderson and M. S. Shive, *Adv. Drug. Deliv. Rev.* **28**, 5 (1997).
18. S.-H. Hyon, *Yonsei Med. J.* **41**, 720 (2000).
19. J. Kreuter, V. E. Petrov, D. A. Kharkevich and R. N. Alyautdin, *J. Control. Rel.* **49**, 81 (1997).
20. A. E. Gulyaev, S. E. Gelperina, I. N. Skidan and A. S. Antropov, *Pharmacol. Res.* **16**, 1564 (1999).

21. S. A. Hagan, A. G. A. Coombes, M. C. Garnett, S. E. Dunn, M. C. Davies, L. Illum and S. S. Davis, *Langmuir* **12**, 2153 (1996).
22. R. K. Kulkarni, K. C. Pani, C. Neaman and F. Leonard, *Arch. Surg.* **93**, 839 (1996).
23. H. S. Choi, T. Ooya, S. Sasaki and N. Yui, *Macromolecules* **36**, 25 (2003).
24. D. Shin, K. Shin, K. A. Aamer, G. N. Tew and T. P. Russell, *Macromolecules* **38**, 104 (2005).
25. W. Z. Yuan, J. Y. Yuan, S. X. Zheng and X. Y. Hong, *Polymer* **48**, 2585 (2007).
26. J. Ren, H. Y. Hong, J. X. Song and T. B. Ren, *J. Appl. Polym. Sci.* **98**, 1884 (2005).
27. H. Fessi, F. Puisieux, J. P. Devissageut, N. Ammoury and S. Benita, *Int. J. Pharm.* **55**, R1 (1989).
28. L. L. Wang and G. Y. Weng, *Chin. J. Pharm.* **31**, 413 (2000).
29. J. Kreuter, *Int. Congr. Ser.* **1277**, 85 (2005).
30. U. Schroeder, P. Sommerfeld, S. Ulrich and B. A. Sabel, *J. Pharm. Sci.* **87**, 1305 (1998).
31. H. F. Wang, Y. Hu, W. Q. Sun and C. S. Xie, *Chin. J. Biotechnol.* **20**, 790 (2004).